First-Principles T-Matrix Theory with Application to the 6 eV Satellite in Ni

M. Springer,[1] F. Aryasetiawan,[1] and K. Karlsson[2]
[1]*Department of Theoretical Physics, University of Lund, Sölvegatan 14A, S-223 62 Lund, Sweden*
[2]*Department of Natural Science, Högskolan i Skövde, 54128 Skövde, Sweden*
(Received 17 September 1997)

In photoemission spectra of strongly correlated systems one usually observes a satellite structure below the main peak. Description of such satellite structures in the commonly used *GW* approximation has been found to be insufficient. To account for these satellite structures that originate from short-range correlations, we have developed a T-matrix formalism for performing *ab initio* calculations on real systems. The method is applied to Ni and we obtain a satellite structure below the Fermi level as well as a reduced exchange splitting. We also found a new interesting satellite structure above the Fermi level, which can be ascribed to particle-particle scattering. [S0031-9007(98)05337-X]

PACS numbers: 71.10.–w, 71.27.+a, 71.28.+d, 71.45.Gm

In many strongly correlated systems, one observes in a photoemission experiment the presence of a satellite structure a few eV below the main peak [1]. The origin of this satellite is due to the presence of two or more holes in a narrow band after a photoelectron is emitted. An illustrative example is provided by Cu and Ni. In Cu, the d band is fully occupied so that after photoemission there is only one d hole in the system corresponding to the $3d^9$ configuration. Since no other holes exist there will be no hole-hole correlation reflected in the absence of a satellite and a single-particle theory is sufficient. On the other hand, the ground state of Ni already contains a configuration with one d hole so that after photoemission, the final state contains a configuration with two d holes. Since the two holes are localized on the same atomic site, there will be a strong d-d interaction resulting in the well-known 6 eV satellite [2–6].

There have been many works studying the electronic structure of highly correlated systems but most of them are based on model Hamiltonians. While they qualitatively provide important insights into the underlying physics, they contain adjustable parameters which hinder a direct quantitative comparison with the experiment.

Ab initio calculations for strongly correlated systems [7,8] have been performed mainly within the *GW* approximation (GWA) [9]. It is known that the GWA works reasonably well in describing the quasiparticle energies but its description of the satellite structure is less satisfactory. Physically, the quasiparticle energies are determined mainly by the long-range screening which is well described within the GWA. Short-range interaction, on the other hand, is not properly described. A natural extension of the GWA is therefore to include short-range correlation which can be described by the T-matrix theory [10–12] which describes multiple scattering between two holes or two particles.

In this Letter we develop a T-matrix theory for performing *ab initio* calculations on real systems. The method is applied to calculate the spectral function of Ni. In the GWA the 6 eV satellite is not obtained. Previous calculations based on Hubbard models showed that the T-matrix theory was capable of yielding a satellite structure in Ni [13–19].

Physically, the T matrix describes multiple scattering between two holes or electrons. It is defined by the following Bethe-Salpeter equation [20]:

$$T_{\sigma_1\sigma_2}(1,2\,|\,3,4) = U(1,2)\,\delta(1-3)\delta(2-4) + U(1,2)\int d1'd2'\,K_{\sigma_1\sigma_2}(1,2\,|\,1',2') \times T_{\sigma_1\sigma_2}(1',2'\,|\,3,4)\,, \tag{1}$$

where U is a screened Coulomb interaction and K is a two-particle propagator. We have used a short-hand notation $1 \equiv (\mathbf{r}_1, t_1)$ and σ labels the spin. Diagrammatically, the multiple scattering processes are shown in Fig. 1.

The kernel K or the two-particle propagator is given by

$$K_{\sigma_1\sigma_2}(1,2\,|\,1',2') = iG_{\sigma_1}(1',1)G_{\sigma_2}(2',2)\,, \tag{2}$$

where G_σ is a time-ordered single-particle Green function. The explicit form of the Fourier transformed kernel K is

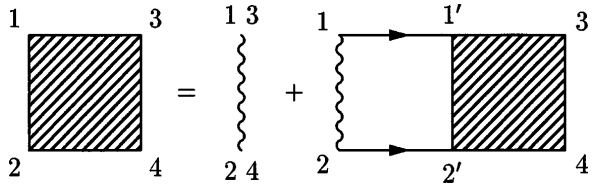

FIG. 1. Feynman diagrams for the T matrix (square): The wiggly and the solid line with the arrow represent the screened interaction U and the Green function G, respectively.

given by

$$K_{\sigma_1\sigma_2}(\mathbf{r}_1,\mathbf{r}_2\,|\,\mathbf{r}'_1,\mathbf{r}'_2;\omega) = -\sum_{ij}^{\text{occ}} \frac{\psi_{i\sigma_1}(\mathbf{r}'_1)\psi^*_{i\sigma_1}(\mathbf{r}_1)\psi_{j\sigma_2}(\mathbf{r}'_2)\psi^*_{j\sigma_2}(\mathbf{r}_2)}{\omega - \varepsilon_{i\sigma_1} - \varepsilon_{j\sigma_2} - i\delta} + \sum_{ij}^{\text{unocc}} \frac{\psi_{i\sigma_1}(\mathbf{r}'_1)\psi^*_{i\sigma_1}(\mathbf{r}_1)\psi_{j\sigma_2}(\mathbf{r}'_2)\psi^*_{j\sigma_2}(\mathbf{r}_2)}{\omega - \varepsilon_{i\sigma_1} - \varepsilon_{j\sigma_2} + i\delta}, \quad (3)$$

where $\psi_{i\sigma}$ is a Bloch state. The first term on the right-hand side is due to hole-hole scattering and the second to particle-particle scattering. This expression is similar to the random-phase approximation (RPA) polarization propagator but the states are either both occupied or unoccupied.

The self-energy obtained from the T matrix consists of a direct term

$$\Sigma^d_{\sigma_2}(4,2) = -i\sum_{\sigma_1}\int d1d3\; G_{\sigma_1}(1,3)T_{\sigma_1,\sigma_2}(1,2\,|\,3,4)\,, \quad (4)$$

and an exchange term

$$\Sigma^x_{\sigma_2}(3,2) = i\int d1d4\; G_{\sigma_2}(1,4)T_{\sigma_2,\sigma_2}(1,2\,|\,3,4)\,. \quad (5)$$

Using the spectral representations of G and T the self-energy can be written explicitly as

$$\text{Im}\,\Sigma^d_{\sigma_2}(\mathbf{r}_4,\mathbf{r}_2;\omega > \mu) = \int d^3r_1d^3r_3 \sum_{\mathbf{k}'n'\sigma_1}^{\text{occ}} \psi_{\mathbf{k}'n'\sigma_1}(\mathbf{r}_1)\psi^*_{\mathbf{k}'n'\sigma_1}(\mathbf{r}_3)\,\text{Im}\,T_{\sigma_1\sigma_2}(\mathbf{r}_1,\mathbf{r}_2\,|\,\mathbf{r}_3,\mathbf{r}_4;\omega + \varepsilon_{\mathbf{k}'n'\sigma_1}) \times \theta(\omega + \varepsilon_{\mathbf{k}'n'\sigma_1} - 2\mu)\,, \quad (6)$$

$$\text{Im}\,\Sigma^d_{\sigma_2}(\mathbf{r}_4,\mathbf{r}_2;\omega \le \mu) = -\int d^3r_1d^3r_3 \sum_{\mathbf{k}'n'\sigma_1}^{\text{unocc}} \psi_{\mathbf{k}'n'\sigma_1}(\mathbf{r}_1)\psi^*_{\mathbf{k}'n'\sigma_1}(\mathbf{r}_3)\,\text{Im}\,T_{\sigma_1\sigma_2}(\mathbf{r}_1,\mathbf{r}_2\,|\,\mathbf{r}_3,\mathbf{r}_4;\omega + \varepsilon_{\mathbf{k}'n'\sigma_1}) \times \theta(-\omega - \varepsilon_{\mathbf{k}'n'\sigma_1} + 2\mu)\,. \quad (7)$$

The screened potential U is in principle frequency dependent. Physically, however, the largest contribution to the T matrix comes from the on site interaction since the d-band width is relatively small. Within the same site, the interaction is essentially instantaneous and therefore it is justified to use an interaction of the form $U(1,2) = U(\mathbf{r}_1,\mathbf{r}_2)\delta(t_1 - t_2)$, where $U(\mathbf{r}_1,\mathbf{r}_2)$ is a static interaction. This static approximation will be used in the present work.

The total self-energy is given by the sum of the GW self-energy and the T-matrix self-energy. However, care must be taken to avoid double counting since the direct second order term in the T matrix is already included in the GWA. A straightforward subtraction of the second order term leads, however, to wrong analytic properties of the self-energy and consequently gives some negative spectral weight. We have constructed a scheme to avoid double counting and to maintain the positive definiteness of the spectral function. This is done by dividing the bare Coulomb interaction into the screened potential U and a long-range part v_L [21]: $v = U + v_L$. The correlation part of the GW self-energy is schematically given by

$$\Sigma^c_{GW} = Gv\,Pv\,, \quad (8)$$

where P is the total RPA response function

$$P = (1 - P^0v)^{-1}P^0, \quad (9)$$

and P^0 is the noninteracting response function. Using the above division of the Coulomb potential we obtain

$$\Sigma^c_{GW} = GUPv_L + Gv_LPU + Gv_LPv_L + GU\,PU\,. \quad (10)$$

The last term is then subtracted off which thereby removes double counting to all orders. It has the same analytic structure as the GW self-energy, but since U is smaller than the bare v, this term is always smaller than the GW self-energy for all frequencies. Numerically it turns out to be very small.

Following the above scheme the total correlation part of the self-energy becomes

$$\Sigma^c_{GWT} = \Sigma^c_{GW} + \Sigma^c_T - GU\,PU\,, \quad (11)$$

where $\Sigma^c_T = \Sigma^d + \Sigma^x$ with Σ^d and Σ^x given by Eqs. (4) and (5), respectively.

Since the T matrix describes scattering between localized holes or particles, it is suitable to work with basis functions which are also localized such as the linear muffin-tin orbitals (LMTO) [22]. In the atomic sphere approximation, the LMTO basis functions are of the form

$$\chi^\sigma_{RL}(\mathbf{r},\mathbf{k}) = \varphi^\sigma_{RL}(\mathbf{r}) + \sum_{R'L'}\dot{\varphi}^\sigma_{R'L'}(\mathbf{r})\,h^\sigma_{R'L',RL}(\mathbf{k})\,. \quad (12)$$

The Bloch states are expanded in the LMTO basis. Using this basis we obtain a matrix equation for T,

$$T_{\sigma\sigma'}(\alpha\beta\,|\,\gamma\delta;\,\omega) = U(\alpha\beta\,|\,\gamma\delta) + \sum_{\eta\nu,\lambda\rho} U(\alpha\beta\,|\,\eta\nu) \times K_{\sigma\sigma'}(\eta\nu\,|\,\lambda\rho;\omega) \times T_{\sigma\sigma'}(\lambda\rho\,|\,\gamma\delta;\omega)\,, \quad (13)$$

which can be easily solved by inversion. We have used a short-hand notation $\alpha \equiv RL$. For practical purposes, we neglect the $\mathbf{k}$ dependence of χ since the largest contribution to K and T arises from the on site term. The Coulomb matrix U is determined from first principles

using the constrained local density approximation (LDA) method [23].

We apply the theory to ferromagnetic Ni. The imaginary part of T exhibits a peak which corresponds to the presence of the so-called "two-hole bound state." The hole created in a photoemission process scatters repeatedly with a virtual hole as in Fig. 1. Since the $3d$-band width is relatively narrow ($\sim$3 eV), two holes on the same site have a small probability to hop from site to site, forming a two-hole state. In a simple single-particle picture, the photoelectron appears to have a smaller kinetic energy since the photon energy is also used to excite a d electron to an empty state above the Fermi level, leaving two holes in the final state. The upper limit for the binding energy is then roughly twice the bandwidth.

To study the spectra as a function of the interaction strength, we use a model potential of the form $U(|\mathbf{r} - \mathbf{r}'|) = \mathrm{erfc}(\alpha|\mathbf{r} - \mathbf{r}'|)/|\mathbf{r} - \mathbf{r}'|$. For the T-matrix self-energy, we notice that the position of the peak in $\mathrm{Im}\,\Sigma_T$ is rather insensitive to the screening parameter. However, the intensity varies with α and consequently the satellite position, which is determined by $\mathrm{Re}\,\Sigma$, is modified accordingly. Thus, if we were allowed to adjust the screening parameter α, the position of the satellite could be shifted arbitrarily. It is therefore crucial to determine the screened interaction U from a parameter-free scheme. According to constrained LDA calculations $U_{dd} \sim 5.5$ eV [17]. Consequently in our calculations we choose $\alpha = 1.2$ which is equivalent to U_{dd} from constrained LDA [24]. Using a different form of U, for example, an exponential, has no effect on the results as long as the screening length is comparable resulting in similar matrix elements.

Our results for the GW self-energies and the T-matrix self-energies for states at the X and Γ points are shown in Figs. 2 and 3, respectively. The double-peak structure in $\mathrm{Im}\,\Sigma_{GW}$ around $\approx$25–30 eV is probably due to plasmon excitations and the peak at $\approx$70 eV is due to the $3p$ core excitation. The T-matrix self-energy has considerable contributions below and above the Fermi level. There is a significant difference between the majority and minority self-energy as can be seen in Figs. 2 and 3. The probability of creating a hole in the majority channel is larger than in the minority channel, since the former is fully occupied. The virtual hole can mainly be created in the minority channel due to the presence of $3d$ unoccupied states just above the Fermi level. This implies that the majority $3d$ self-energy will be larger than the minority one which reduces the exchange splitting, which in the LDA and GWA is too large (0.6 eV vs 0.3 eV experimentally). Consequently, the GW-band width, which is too large by $\approx$0.4 eV [7], is also improved.

Our calculated spectral functions for states at the X and Γ points are displayed in Figs. 4 and 5, respectively. The main peak $\sim$3 eV below the Fermi level is the quasiparticle peak. A satellite structure originating from the T-matrix self-energy, absent in the GWA, can be observed

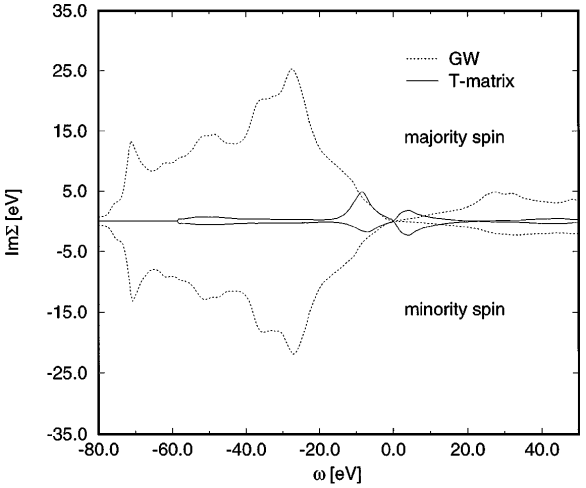

FIG. 2. Imaginary part of Σ for Ni at the X point corresponding to the second occupied state. The full line is the T-matrix contribution and the dotted line the GW contribution.

below the main peak. The satellite starts indeed at $\approx$6 eV and the shape compares well with the experiment [2,5] although the main peak is somewhat lower than the experimental one. One possible reason for this is the neglect of particle-hole scattering which should reduce the satellite binding energy. Moreover, the true value of U may be smaller than the one used in the present work.

The intensity of the satellite peak varies through the d band, being largest for states at the bottom of the band. As a consequence, the bottom of the $3d$ band is most affected by the T matrix resulting in a decrease in the band width of $\approx$0.3 eV. This decrease is significantly smaller than what was found in model calculations [14] pointing to the importance of matrix elements neglected in Hubbard models. The exchange splitting experiences the largest

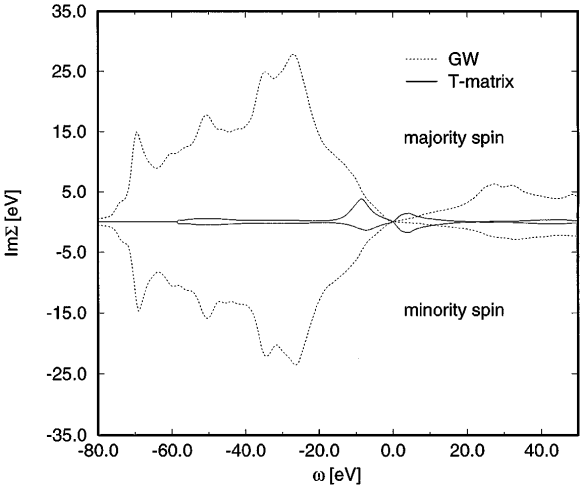

FIG. 3. Imaginary part of Σ for Ni at the Γ point corresponding to the second occupied state. The full line is the T-matrix contribution and the dotted line the GW contribution.

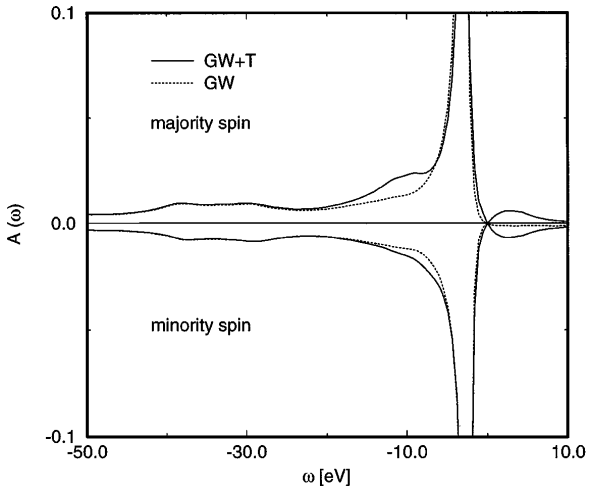

FIG. 4. Ni spectral function for the second occupied state (d band) at the X point.

reduction also for states at the bottom of the $3d$ band by ≈ 0.3 eV.

An interesting new feature is the presence of a peak structure just above the Fermi energy which arises from particle-particle scattering. At first sight, these scattering processes are expected to be insignificant, since the number of unoccupied states is small which leads to a small T matrix for positive energies. However, there is a sum over occupied states which amplifies the small contribution from the T matrix as can be seen in Eq. (6). It should be possible to measure this satellite structure in an angular resolved inverse photoemission experiment by choosing certain $\mathbf{k}$ vectors, where the quasiparticle peak is well separated from the satellite.

In summary, to describe short-range correlations neglected in the GWA, we have developed an *ab initio* T-matrix theory for real systems, which takes into account band structure effects and spin-spin correlations neglected in the GWA. This represents a first step towards an *ab initio* scheme for strongly correlated systems which was not available before. The method is applied to Ni giving a satellite structure below the main quasiparticle peak corresponding to the 6 eV satellite and reducing the exchange splitting as well as improving the GW-band width. In addition, we found a new satellite structure just above the Fermi level. These encouraging results motivate further applications to more complex systems such as transition metal monoxides.

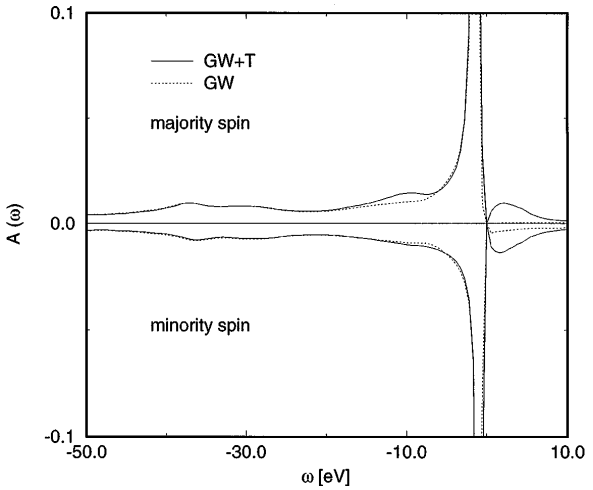

FIG. 5. Ni spectral function for the second occupied state (d band) at the Γ point.

[1] S. Hüfner, *Photoelectron Spectroscopy*, Springer Series in Solid-State Sciences Vol. 82 (Springer-Verlag, Berlin/Heidelberg, 1996).
[2] S. Hüfner, G. K. Wertheim, N. V. Smith, and M. M. Traum, Solid State Commun. **11**, 323 (1972).
[3] C. Guillot, Y. Ballu, J. Paigné, J. Lecante, K. P. Jain, P. Thiry, R. Pinchaux, Y. Pétroff, and L. M. Falicov, Phys. Rev. Lett. **39**, 1632 (1977).
[4] R. J. Smith, J. Anderson, J. Hermanson, and G. J. Lapeyre, Solid State Commun. **21**, 459 (1977).
[5] F. J. Himpsel, J. A. Knapp, and D. E. Eastman, Phys. Rev. B **19**, 2919 (1979).
[6] J. Kanski, P. O. Nilsson, and C. G. Larsson, Solid State Commun. **35**, 397 (1980).
[7] F. Aryasetiawan, Phys. Rev. B **46**, 13 051 (1992).
[8] F. Aryasetiawan and O. Gunnarsson, Phys. Rev. Lett. **74**, 3221 (1995).
[9] L. Hedin and S. Lundqvist, in *Solid State Physics*, edited by H. Ehrenreich, F. Seitz, and D. Turnbull (Academic, New York, 1969), Vol. 23, p. 1.
[10] J. Kanamori, Prog. Theor. Phys. **30**, 275 (1963).
[11] H. Suehiro, Y. Ousaka, and H. Yasuhara, J. Phys. C **19**, 4247 (1986); *ibid.* **19**, 4263 (1986).
[12] H. Yasuhara, H. Suehiro, and Y. Ousaka, J. Phys. C **21**, 4045 (1988).
[13] D. R. Penn, Phys. Rev. Lett. **42**, 921 (1979).
[14] A. Liebsch, Phys. Rev. B **23**, 5203 (1981).
[15] G. Treglia, F. Ducastelle, and D. Spanjaard, Phys. Rev. B **21**, 3729 (1980).
[16] C. Calandra and F. Manghi, Phys. Rev. B **45**, 5819 (1992).
[17] M. M. Steiner, R. C. Albers, and L. J. Sham, Phys. Rev. B **45**, 13 272 (1992).
[18] Jun-ichi Igarashi, P. Unger, K. Hirai, and P. Fulde, Phys. Rev. B **49**, 16 181 (1994).
[19] F. Manghi, V. Bellini, and C. Arcangeli, Phys. Rev. B **56**, 7149 (1997).
[20] See, e.g., A. L. Fetter and J. D. Walecka, *Quantum Theory of Many-Particle Systems* (McGraw-Hill, New York, 1971).
[21] Ulf von Barth (private communication).
[22] O. K. Andersen, Phys. Rev. B **12**, 3060 (1975).
[23] O. Gunnarsson, O. K. Andersen, O. Jepsen, and J. Zaanen, Phys. Rev. B **39**, 1708 (1989).
[24] M. Springer and F. Aryasetiawan, Phys. Rev. B (to be published).